

# High-Throughput Cytochrome P450 Inhibition Assays Using Laser Diode Thermal Desorption-Atmospheric Pressure Chemical Ionization-Tandem Mass Spectrometry

Jin Wu,<sup>†</sup> Christopher S. Hughes,<sup>†</sup> Pierre Picard,<sup>‡</sup> Sylvain Letarte,<sup>‡</sup> Mireille Gaudreault,<sup>†</sup> Jean-François Lévesque,<sup>†</sup> Deborah A. Nicoll-Griffith,<sup>†</sup> and Kevin P. Bateman<sup>\*,†</sup>

Merck Frosst Centre for Therapeutic Research, 16711 Trans Canada Highway, Kirkland, QC, Canada H9H 3L1, and  
Phytronix Technologies Inc., 337 Rue Saint-Joseph East, Québec, QC, Canada G1K 3B3

This paper describes the development of a high-throughput method for the analysis of cytochrome P450 (CYP) inhibition assay incubation samples using laser diode thermal desorption interfaced with atmospheric pressure chemical ionization mass spectrometry (LDTD-APCI-MS). Data for the CYP isoforms 3A4, 2D6, 2C9, and 1A2 from competitive inhibition assays are shown. The potential for inhibition of the CYP isoforms was measured by monitoring the level of the metabolites 6 $\beta$ -hydroxytestosterone (3A4), dextrophan (2D6), 4'-hydroxydiclofenac (2C9), and acetaminophen (1A2) formed in the presence of drug candidates using an eight-point titration. The analytical method involves plating of the inhibition samples on specially designed 96-well plates with stainless steel bottoms, followed by direct analysis using the LDTD source. Validation of the LDTD-MS method was performed by testing for interferences, reproducibility, dynamic range, ion suppression, and the ability of the source to produce comparable results to previously validated LC-MS methods. IC<sub>50</sub> values for each CYP isoform using 33 different test compounds showed excellent agreement between LDTD-APCI-MS and LC-MS methods and literature values where available. Assay analysis time using the LDTD-APCI source is reduced to less than 30 min for a single 96-well plate compared to greater than 10 h using the LC-MS method. The LDTD-APCI-MS and LC-MS methods and results are compared and limitations and future potential for LDTD-APCI-MS are discussed.

Screening during early drug discovery to identify potential liabilities of drug candidates is a widespread practice in the pharmaceutical industry.<sup>1</sup> This is especially true for properties that could result in drug-drug interactions. The largest contributing factor to the occurrence of drug-drug interactions is inhibition of the cytochrome P450 (CYP) family of enzymes.<sup>2</sup> This super-

family of membrane-bound heme proteins is responsible for the oxidative metabolism of a wide variety of endobiotics and xenobiotics.<sup>3–6</sup> There are a large number of different CYP families and isoforms found in humans, the CYP3A family being the most commonly studied.<sup>6,7</sup> Competitive CYP inhibition assays are regularly used to determine the effect a drug candidate may have on CYP-mediated metabolism of selected probe substrates.<sup>8–12</sup> CYP inhibitors can compromise the pharmacokinetics, efficacy, and safety profile of coadministered drugs and often cause undesired or even fatal adverse effects.<sup>3,4,6</sup>

CYP inhibition assays are performed in vitro using human liver-based systems. Assays commonly use recombinant enzymes, microsomal subcellular fractions, or hepatocytes, as sources of CYP enzymes.<sup>12</sup> Human hepatic microsomes are prepared from homogenized liver tissue that has been separated through ultracentrifugation into microsomal, S9, mitochondrial, and cytosolic fractions.<sup>3</sup> Microsomes are commonly used due to their ease of use and maintenance, stability, and the high concentration of CYP enzymes the microsomes contain.<sup>3</sup> Typical CYP inhibition assays are performed using human liver microsomes (HLM) in the presence of a specific CYP probe substrate, NADPH, and a range of test compound concentrations.

Conventional methods of screening drug candidates for CYP inhibition involve the use of LC-MS, HPLC-UV, fluorescence, and radioactivity-based methods.<sup>10,11,13–20</sup> Fluorometric assays can

\* To whom correspondence should be addressed. Phone: (514) 428-8689. Fax: (514) 428-8615. E-mail: Kevin\_Bateman@merck.com.

<sup>†</sup> Merck Frosst Centre for Therapeutic Research.

<sup>‡</sup> Phytronix Technologies Inc.

(1) Ekins, S.; Ring, B. J.; Grace, J.; McRobie-Belle, D. J.; Wrighton, S. A. *J. Pharmacol. Toxicol. Methods* **2000**, *44*, 313–324.

(2) Yamamoto, T.; Suzuki, A.; Kohno, Y. *Xenobiotica* **2003**, *33*, 823–839.

(3) Ansedé, J. H.; Thakker, D. R. *J. Pharm. Sci.* **2004**, *93*, 239–255.

(4) Testino, S. A., Jr.; Patonay, G. *J. Pharm. Biomed. Anal.* **2003**, *30*, 1459–1467.

(5) Rendic, S.; Di Carlo, F. J. *Drug Metab. Rev.* **1997**, *29*, 413–580.

(6) Yin, H.; Racha, J.; Li, S.-Y.; Olejnik, N.; Satoh, H.; Moore, D. *Xenobiotica* **2000**, *30*, 141–154.

(7) Ekins, S.; Stresser, D. M.; Williams, J. A. *Trends Pharmacol. Sci.* **2003**, *24*, 161–166.

(8) Palamanda, J. R.; Favreau, L.; Lin, C.-C.; Nomeir, A. A. *Drug Discovery Today* **1998**, *3*, 466–470.

(9) Saraswat, L. D.; Caserta, K. A.; Laws, K.; Wei, D.; Jones, S. S.; Adedoyin, A. *J. Biomol. Screening* **2003**, *8*, 544–554.

(10) Di Marco, A.; Marcucci, I.; Chaudhary, A.; Taliani, M.; Laufer, R. *Drug Metab. Dispos.* **2005**, *33*, 359–364.

(11) Di Marco, A.; Marcucci, I.; Verdirmé, M.; Pérez, J.; Sanchez, M.; Peláez, F.; Chaudhary, A.; Laufer, R. *Drug Metab. Dispos.* **2005**, *33*, 349–358.

(12) Rodrigues, A.; Lin, J. *Curr. Opin. Chem. Biol.* **2001**, *5*, 396–401.

(13) Lin, J. H.; Lu, A. Y. H. *Clin. Pharmacokinet.* **1998**, *35*, 361–390.

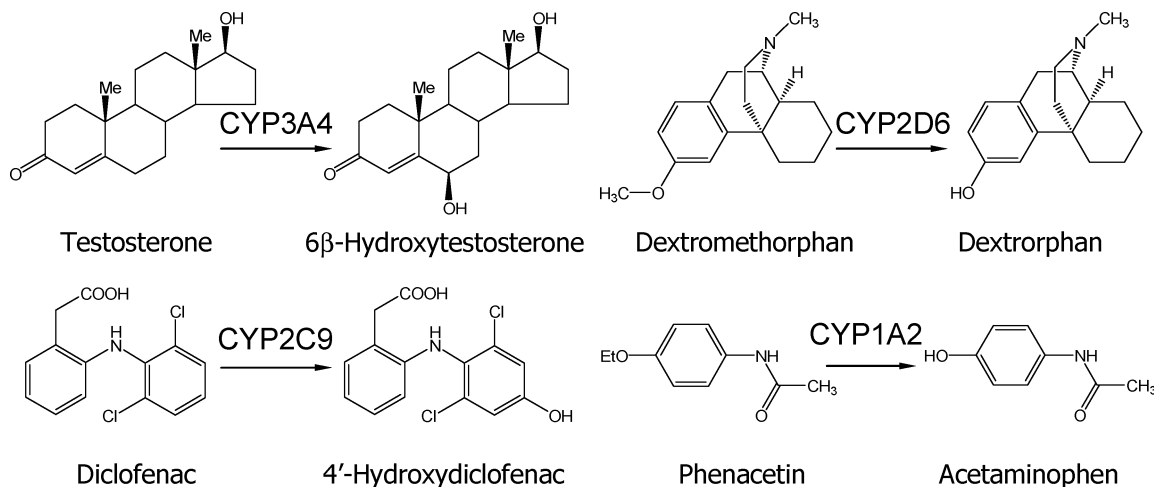


**Figure 1.** Structures of cytochrome P450 probes and metabolites.

suffer from lack of probe specificity, consequently recombinant CYPs have to be used. Furthermore, test compounds or metabolites that are fluorescent can cause interference, thereby limiting the general use of fluorescent probes. Radiometric assays, while not prone to the shortcomings of fluorescent assays, are less cost-effective because of expensive reagents and waste disposal. LC-MS, because of its high sensitivity and high selectivity, is the most commonly used method for analyzing CYP inhibition assay samples. All of the detection methods monitor the amount of metabolite formed from the probe substrate by the CYP isoform in the presence of different concentrations of drug candidate. LC-MS commonly represents the bottleneck in the CYP inhibition assay. A number of LC methodologies such as multiple columns, full system automation, peak stacking, monolithic columns, and cocktail probes or sample pooling combined with fast gradient have all been tested in attempts to reduce the run time.<sup>18–24</sup>

Here we report the development and application of a laser diode thermal desorption (LDTD) sample introduction source coupled with atmospheric pressure chemical ionization (APCI) and tandem mass spectrometry (MS/MS) to the high-throughput analysis of CYP 1A2/2C9/2D6/3A4 inhibition assays. Thermal desorption is a method for generating gas-phase molecules from

samples that have been adsorbed onto a surface, and APCI is the technique for transforming neutral gas-phase molecules into ions for analysis by mass spectrometry. The LDTD source uses an infrared laser to thermally desorb samples that have been dried onto stainless steel sample wells in a 96-well plate. In LDTD-APCI-MS, the desorbed gas-phase molecules pass by a corona discharge needle, which results in ionization prior to analysis in a mass spectrometer.<sup>25</sup> LDTD-APCI-MS offers decreased sample analysis times when compared to currently available LC-MS-based methods and offers a new avenue for high-throughput analysis. A comparison of the LDTD-APCI-MS with a validated LC-MS-based method is made. Future prospects for the LDTD source are discussed, as well as potential limitations.

## MATERIALS AND METHODS

**Materials.** 6 $\beta$ -Hydroxytestosterone, testosterone, dextromethorphan, diclofenac, phenacetin, equilin, flufenamic acid, acetaminophen, diltiazem, flutamide, fluvoxamine, sulfaphenazole, miconazole, genistein, zafirlukast, ketoconazole, nifedipine, imipramine, desipramine, clozapine, bufuralol, mifepristone,  $\alpha$ -naphthoflavone, nicardipine, and  $\beta$ -nicotinamide adenine dinucleotide phosphate reduced tetrasodium salt (NADPH) were obtained from Sigma-Aldrich Chemical Co. (St. Louis, MO). 4'-Hydroxydiclofenac, [<sup>13</sup>C<sub>2</sub>, <sup>15</sup>N]-acetaminophen, [D<sub>3</sub>]-dextrorphan, and the 20 mg/mL HLM protein stock solutions (lot 23) were all obtained from BD Gentest (Woburn, MA). [16,16,17-D<sub>3</sub>]-6 $\beta$ -Hydroxytestosterone was obtained from Cerilliant (Round Rock, TX). Dextrorphan was obtained from RBI. [Dichlorophenol-U-<sup>13</sup>C<sub>6</sub>]-4'-hydroxydiclofenac was synthesized at Merck Research Laboratories. Clarithromycin was purchased from Sequoia Research Products (Pangbourne, UK). Monobasic sodium phosphate was purchased from Anachemia (Montreal, QC, Canada). HPLC gradient acetonitrile and formic acid (99.9%) were obtained from commercial sources and used without further purification. Industrial grade gases and deionized water were used throughout.

**Competitive CYP1A2//2D6/2C9/3A4 Inhibition Assays.** Competitive inhibition assays measuring the CYP isozymes 1A2, 2C9, 2D6, and 3A4 were prepared in separate 300- $\mu$ L round-bottom 96-well plates (Costar, Fisher, Nepean, ON, Canada). Figure 1

- (14) Moody, G. C.; Griffin, S. J.; Mather, A. N.; McGinnity, D. F.; Riley, R. J. *Xenobiotica* **1999**, *29*, 53–75.
- (15) Chauret, N.; Tremblay, N.; Lackman, R. L.; Gauthier, J.-Y.; Silva, J. M.; Marois, J.; Yergey, J. A.; Nicoll-Griffith, D. A. *Anal. Biochem.* **1999**, *276*, 215–226.
- (16) Cali, J. J.; et al. Luminescence-based methods and probes for measuring cytochrome P450 activity. Promega Corp. USP application 20040171099, 2004.
- (17) Crespi, C. L.; Miller, V. P.; Penman, B. W. *Anal. Biochem.* **1997**, *258*, 188–190.
- (18) Bhoopathy, S.; Xin, B.; Unger, S. E.; Karnes, H. T. *J. Pharm. Biomed. Anal.* **2005**, *37*, 739–749.
- (19) Peng, S. X.; Barbone, A. G.; Ritchie, D. M. *Rapid Commun. Mass Spectrom.* **2003**, *17*, 509–518.
- (20) Ayrtton, J.; Plumb, R.; Leavens, W. J.; Mallett, D.; Dickinson, M.; Dear, G. J. *Rapid Commun. Mass Spectrom.* **1998**, *12*, 217–224.
- (21) Chu, I.; Favreau, L.; Soares, T.; Lin, C.-C.; Nomeir, A. A. *Rapid Commun. Mass Spectrom.* **2000**, *14*, 207–214.
- (22) Bu, H.-Z.; Magis, L.; Knuth, K.; Teitelbaum, P. *Rapid Commun. Mass Spectrom.* **2000**, *14*, 1619–1624.
- (23) Janiszewski, J. S.; Rogers, K. J.; Whalen, K. M.; Cole, M. J.; Liston, T. E.; Duchoslav, E.; Fouda, H. G. *Anal. Chem.* **2001**, *73*, 1495–1501.
- (24) Kim, M.-J.; Kim, H.; Cha, I.-J.; Park, J.-S.; Shon, J.-H.; Liu, K.-H.; Shin, J.-G. *Rapid Commun. Mass Spectrom.* **2005**, *19*, 2651–2658.

(25) www.phytronix.com.

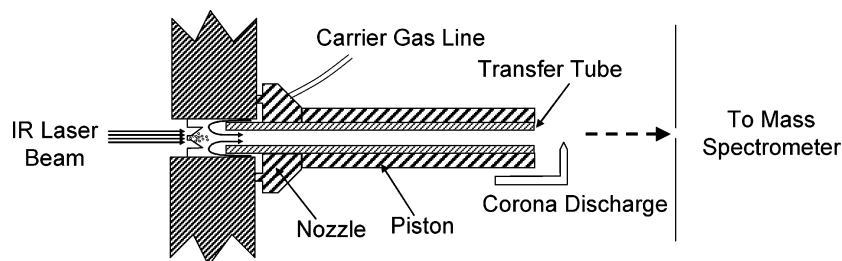


**Figure 2.** Schematic of the LDTD source.

shows the structures of the CYP probes used in this study and their corresponding metabolites. Probe stock solutions of 2.5 mM testosterone, 0.75 mM dextromethorphan, 0.5 mM diclofenac, and 5 mM phenacetin were prepared in acetonitrile. The 0.25 and 0.5 mg/mL HLM protein solutions were prepared in a pH 7.4 phosphate buffer from the BD-Gentest Lot 23 HLM. The 0.25 mg/mL HLM protein was used in the CYP 2C9, 2D6, and 3A4 assays while the 0.5 mg/mL HLM protein solution was used in the CYP 1A2 assay. A quenching solution containing 40% acetonitrile and 0.05% formic acid was prepared in water. The internal standards used in the assay along with their concentrations in the individual quenching solution were as follows: CYP 1A2, 1  $\mu$ M [ $^{13}\text{C}_2$ ,  $^{15}\text{N}$ ]-acetaminophen, CYP2C9, 15  $\mu$ M [dichlorophenol- $\text{U-}^{13}\text{C}_6$ ]-4'-hydroxydiclofenac, CYP2D6, 4  $\mu$ M [ $\text{D}_3$ ]-dextropropan, and CYP3A4, 10  $\mu$ M [16,16,17- $\text{D}_3$ ]-6 $\beta$ -hydroxytestosterone. Metabolite stock solutions of acetaminophen, 4'-hydroxydiclofenac, dextropropan, and 6 $\beta$ -hydroxytestosterone were each prepared at concentrations ranging from 500  $\mu$ M to as low as 2  $\mu$ M. The stock solution of 20 mg/mL NADPH was freshly prepared in the pH 7.4 phosphate buffer. Plates were prepared by sequentially adding HLM, probe substrate (final concentration 1A2 100  $\mu$ M, 2C9 10  $\mu$ M, 2D6 15  $\mu$ M, 3A4 50  $\mu$ M), test compound (0.03, 0.01, 0.3, 0.1, 3, 10, 30, 100  $\mu$ M final concentration), and NADPH (1 mM in incubation) to a 300- $\mu$ L round-bottom 96-well plate using a Biomek 2000 robotic system (Beckman Coulter, Mississauga, ON, Canada). The incubation volume was 100  $\mu$ L in each well. The plate design also contained appropriate controls, including maximum turnover control, minimum turnover control, ion suppression control, and metabolite standard curve. The CYP3A4 and 2C9 plates were incubated for 10 min, and the 2D6 and 1A2 plates for 20 min at 37  $^\circ\text{C}$ . The incubations were then quenched with an equal volume of the quenching solution containing internal standard using a Multimek 96 (Beckman Coulter), followed by centrifugation at 4000 rpm for 10 min. The 1A2, 2C9, 2D6, and 3A4 plates were pooled to a single plate and diluted 12 $\times$  with water for LC-MS analysis. For LDTD-MS analysis, 20- $\mu$ L samples from individual incubation plate were diluted 5 $\times$  with acetonitrile. Aliquots of 2  $\mu$ L were transferred from the dilution plate to a LazWell 96-well plate (Phytronix Technologies, Quebec, QC, Canada) using a Biomek 2000 FX robot (Beckman Coulter). The samples were allowed to dry under  $\text{N}_2$  and were subjected to LDTD-APCI-MS/MS analysis.

**CYP3A4 Antibody Incubations.** Incubations were conducted in 1.5-mL Eppendorf tubes. The samples were prepared in duplicate using two separate concentrations of HLM protein, 0.25 and 1 mg/mL. Two antibodies were tested, a control antibody

and an anti-CYP3A4 monoclonal antibody (mAB).<sup>26</sup> Incubations were prepared by combining a pH 7.4 phosphate buffer, HLM, and the specified antibody or no antibody (phosphate buffer) and placed on ice for 15 min. The substrate, i.e., testosterone, was added to the mixture with a final concentration of 50  $\mu$ M. NADPH was then added to initiate the enzymatic reaction, and the samples were incubated for 10 min in a 37  $^\circ\text{C}$  water bath. The incubation volume was 200  $\mu$ L with 1% of organic content. Samples were then quenched with 200  $\mu$ L of acetonitrile followed by centrifugation (10 min, 4000 rpm) and a further dilution of the supernatant with an equal volume of water. The samples were then analyzed using UPLC/QTOF-MS (Waters, Milford, MA).

**Instrumental Information.** LC-MS/MS analysis of competitive CYP inhibition assays was conducted on a PE Sciex API 2000 triple quadrupole LC-MS/MS instrument controlled by Analyst software 1.4.1 (Concord, ON, Canada). The LC system consisted of Shimadzu pumps, controller, and autosampler (Kyoto, Japan). The mobile phases were composed of 0.1% formic acid in water (A) and 0.1% formic acid in acetonitrile (B), flowing at 0.3 mL/min. The LC column was an Eclipse XDB  $\text{C}_{18}$  2.1  $\times$  50 mm, 1.8- $\mu$ m column from Agilent (Palo Alto, CA).

The LDTD source was developed and manufactured by Phytronix Technologies (Quebec, QC, Canada). The source was mounted on an API 4000 triple quadrupole mass spectrometer (Applied Biosystems/MDS Sciex) using a replica of the TurboV source mounting mechanism. The assembly contained an infrared diode laser (980 nm, 20 W, continuous) with an X-Y moveable stage capable of holding one LazWell 96-well plate, a piston, a transfer tube made of stainless steel, and a corona discharge needle (Figure 2). The LazWell plate was in the 96-well plate format made of polypropylene with the inserts made of proprietary stainless steel alloy. Upon operation, the plunger powered by nitrogen inserts into a sample well, the programmable laser thermally desorbs the dried sample (2  $\mu$ L spotted) by heating the back of the plate, and the desorbed neutral sample is passed by the carrier gas (medical grade air) along the transfer tube to the corona discharge needle to be ionized and then transmitted into the MS. The LDTD source used the following settings: corona discharge voltage 5500 V, turbo gas temperature 22  $^\circ\text{C}$ , entrance potential 10 V, curtain gas 10, nebulizing gas 0, and turbo gas 0. In most of the experiments, the carrier gas flowed at a rate of 2.25 L/min and laser power was ramped from 0 to 70% over 1 s and held at 70% power for 5 s before shutting off.

(26) Mei, Q.; Tang, C.; Assang, C.; Lin, Y.; Slaughter, D.; Rodrigues, A. D.; Baillie, T. A.; Rushmore, T. H.; Shou, M. *J. Pharmacol. Exp. Ther.* **1999**, 291, 749–59.



**Table 1. Optimized LDTD-APCI-MS Conditions for CYP Probe Metabolites and Internal Standards**

compound	laser power, carrier gas flow rate, and temperature	Q1, <i>m/z</i>	Q3, <i>m/z</i>	DP (V)	CE (eV)	CXP (V)
6 $\beta$ -hydroxytestosterone	0–70% in 1 s, 70% for 5 s 2–2.5 L/min, 50 °C	305.3	269.1	60	20	15
[16,16,17- $D_3$ ]-6 $\beta$ -hydroxytestosterone		308.4	272.1			
dextrorphan		258.3	201.0			
[ $D_3$ ]-dextrorphan		261.0	201.0	80	43	6
4'-hydroxydiclofenac		312.2	231.1			
[ $^{13}C_6$ ]-4'-hydroxydiclofenac		320.1	238.8			
acetaminophen		152.0	110.2			
[ $^{13}C_2$ , $^{15}N$ ]-Acetaminophen		154.8	111.0			

For LDTD-APCI-MS/MS, sample optimization was first performed by direct infusion of 5  $\mu$ M standard samples using the standard ESI source to obtain the correct transitions for SRM scans. The TurboV ESI source used the following source conditions in the positive mode: ion spray voltage 5500 V, turbo gas temperature 600 °C, entrance potential 10 V, nebulizing gas 30, and turbo gas 30. The LDTD source parameters were then optimized using the defined SRM scans. After the optimal LDTD parameters were obtained, a reoptimization of MS and MS/MS conditions was performed using the LDTD source directly. Spotted standards were used to obtain more specific SRM parameters for the LDTD source. The standards spotted on the LazWell plates were 2  $\mu$ L of 5  $\mu$ M standards of all probe metabolites and internal standards shot in triplicate for each of MS and MSMS scans. The optimized method conditions such as laser power, carrier gas flow, Q1/Q3 SRM transitions, declustering potential (DP), collision energy (CE), and collision cell exit potential (CXP) for the LDTD-MS/MS system are summarized in Table 1.

CYP3A4 antibody incubation samples were analyzed using an Acquity UPLC system interfaced with a Q-TOF Premier mass spectrometer controlled by MassLynx 4.0. The LC separation was achieved with an Acquity UPLC BEH  $C_{18}$  column (1.7  $\mu$ m, 50  $\times$  2.1 mm) operated at 60 °C. Mobile phase A was 0.1% formic acid in water and mobile phase B was 0.1% formic acid in acetonitrile with a total flow rate of 0.5 mL/min. Mobile phase B was linearly ramped from 10 to 20% in 1.9 min, held at 20% for 0.1 min, ramped to 50% in 2.5 min and then to 90% in 0.01 min, held at 90% for 0.4 min, and then immediately stepped back to 10% for re-equilibration. The Q-TOF Premier was operated in the MS scan mode under the following conditions: mass range 100–500 amu, capillary voltage 3.3 kV, cone voltage 30 V, collision energy 10 eV, source temperature 120 °C, desolvation temperature 350 °C, cone gas flow 20 L/h, and desolvation gas flow 600 L/h.

**Software Control and Data Analysis.** The LC–MS data and LDTD-MS data were acquired and analyzed using Analyst 1.4.1 software. The LDTD source was controlled by LazSoft 2.0 software developed by Phytronix Technologies. The LC–MS data were acquired conventionally, such that each sample well had its own data file, and all the data were quantified by the Analyst quantitation software. In contrast, the LDTD-MS data for one 96-well plate was acquired into a single data file. The LazSoft program allows for acquisition into individual files if preferred. Automatic peak integration was performed using the Analyst IntelliQuan algorithm or the MaldiQuan software (MDS Sciex). Data were exported from Analyst and imported into a specifically designed data analysis program at Merck Frosst (Kirkland, QC, Canada)

for further analysis. Inhibition curves and IC<sub>50</sub> values (concentration of an inhibitor that is required for 50% inhibition of an enzyme *in vitro*) were generated using the in-house-developed software.

## RESULTS AND DISCUSSION

**Principles of LDTD.** LDTD is a new sample introduction technique combining thermal desorption and APCI.<sup>25</sup> A small amount of sample (1–10  $\mu$ L) is deposited into the wells of the LazWell plate without applying any matrix and then allowed to dry or dried using a gentle stream of N<sub>2</sub> gas. The LazWell plate is designed as a conventional 96-well plate, which is made of high-density polypropylene with proprietary stainless steel inserts as the well bottom. The inserts are hexagonal in the center to facilitate sample deposition. The plate is held in an *X–Y* stage that positions it in alignment with the laser. The flare-shaped portion of the nozzle abuts on the LazWell plate while the transfer tube is driven by a pneumatic piston into the sample well. Thermal desorption is produced by an infrared laser diode (980 nm, 20 W) that is focused sequentially at the back of each well. A fast ramp in temperature causes sample desorption to form gaseous neutral molecules. The gaseous sample is carried by the preheated carrier gas through the transfer tube, ionized by corona discharge-induced chemical ionization, and introduced directly into the mass spectrometer. A schematic of the source is shown in Figure 2.

The optimal vaporization of an analyte is governed by two major variables: maximum heating temperature and heating time. The temperature must be sufficiently high to desorb the sample, but not so high that it induces thermal fragmentation. The analyte should leave the surface quickly to avoid excess energy transfer that may cause thermal degradation. Unlike matrix-assisted laser desorption/ionization, LDTD requires no matrix, desorption is caused by indirect heating, and the ionization process is decoupled from generation of gas-phase molecules.

**Characterization of the LDTD Source.** The LDTD source requires that three user-defined parameters be optimized for each sample before an effective analysis can take place, these being laser power and duration and the carrier gas flow rate. Laser power was optimized using individual metabolites and internal standards at 5  $\mu$ M in protein-precipitated human liver microsomes. Each sample was analyzed in triplicate from 10 to 100% laser power in steps of 10%. Figure 3a displays an example of laser power optimization for 4'-hydroxydiclofenac. The optimal laser power was chosen from the average peak area values of the triplicate samples, along with the optimal peak shape and reproducibility. Carrier gas flow rate was optimized by analyzing the standards in replicates of five while varying the flow rate from 0.5 to 3.5 L/min

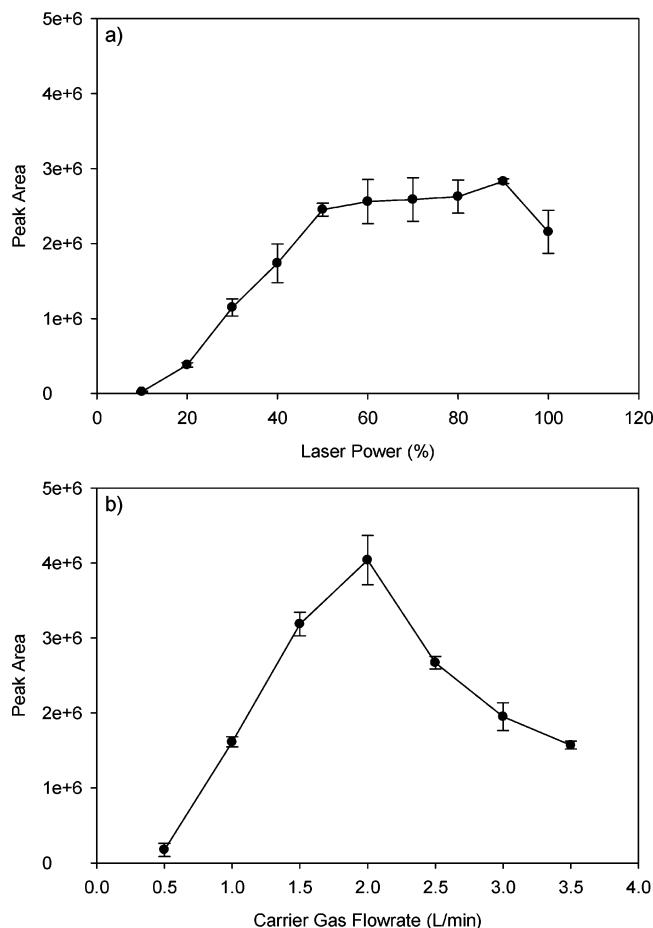


**Figure 3.** LDTD optimization for 4'-hydroxydiclofenac. (a) Peak area versus laser power with the carrier gas flow rate set at 2 L/min. (b) Peak area versus gas flow rate with the laser power set at 90%.

in steps of 0.5 L/min. Figure 3b shows an example of flow rate optimization for 4'-hydroxydiclofenac. The optimal laser power obtained from the previous experiment was used when optimizing the flow rate. Optimal flow rate was chosen by comparison of the average peak area, peak shape, and reproducibility of the five samples. The final laser power and flow rate of 70% and 2.25 L/min was chosen as a compromise to optimize the sensitivity of all samples. Optimal desorption time was set at 5 s in order to desorb the entire sample while allowing for fast well-to-well analysis time.

Analysis of a 96-well sample plate containing 2- $\mu$ L spots of 5  $\mu$ M 6 $\beta$ -hydroxytestosterone and 5  $\mu$ M [16,16,17-D<sub>3</sub>]-6 $\beta$ -hydroxytestosterone in a HLM solution was tested in order to determine the % RSD from well to well. The plate showed a peak area RSD of 10% for 6 $\beta$ -hydroxytestosterone with no internal standard correction and <8% with internal standard correction. To test the dynamic range and sensitivity capabilities of the LDTD source, calibration standards prepared in protein-precipitated HLM at concentrations from 1.28 nM to 20  $\mu$ M in dilution steps of 5-fold were analyzed individually. 6 $\beta$ -Hydroxytestosterone showed a linear range of 1.28 nM–20  $\mu$ M with an LOD of 1 nM. Dextrorphan and 4'-hydroxydiclofenac showed a linear range of 1.28 nM–4  $\mu$ M with a calculated LOD of <1 nM. Acetaminophen was linear from 6.4 nM to 4  $\mu$ M with an LOD of ~6 nM.  $R^2$  values for 6 $\beta$ -hydroxytestosterone, dextrorphan, 4'-hydroxydiclofenac, and acetaminophen were 0.9991, 0.9989, 0.9949, and 0.9892, respectively. Calibration was also examined in the same concentration

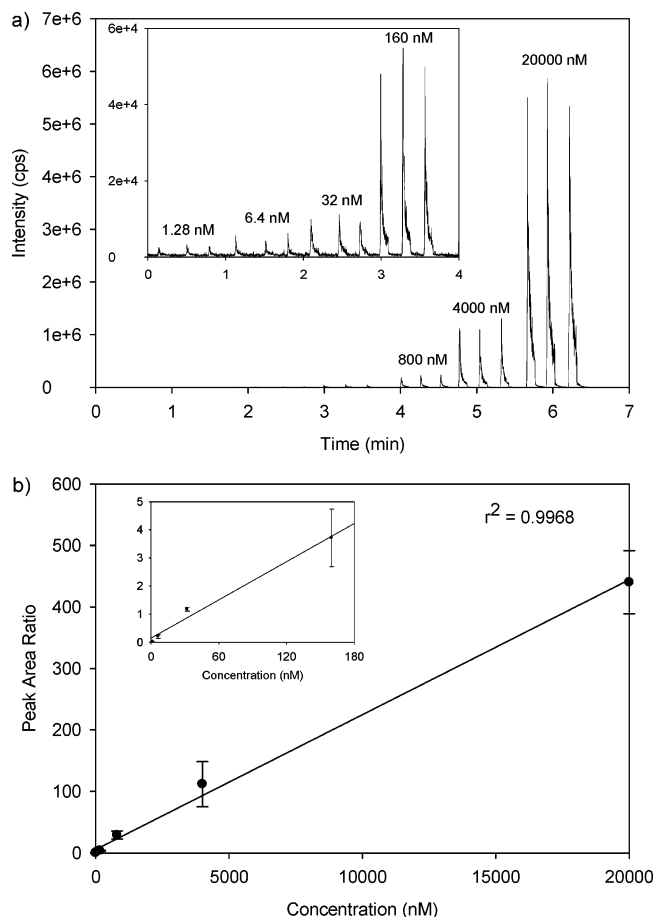


**Figure 4.** Calibration curve of 6 $\beta$ -hydroxytestosterone in the mixture of all the analytes and internal standards in a 0.25 mg/mL HLM protein solution (protein precipitated with equal volume of acetonitrile). (a) LDTD-APCI-MS raw data showing samples from 1.28 nM to 20  $\mu$ M in triplicate (21 wells in 7 min). (b) Calibration curve plot for the data shown in panel a.

range with all analytes and internal standards prepared in a single mixture. Minimal loss of sensitivity was observed for the mixed samples, and linearity was excellent. Figure 4 shows the extracted ion current trace and the calibration curve for 6 $\beta$ -hydroxytestosterone in the mixture.

CYP inhibition assays typically use LC–MS detection with either ESI or APCI. Table 2 shows a comparison of ESI, APCI, and LDTD peak areas and signal-to-noise (S/N) ratios for the four probe metabolites (5  $\mu$ M) prepared in 0.25 mg/mL HLM protein solutions (protein precipitated with equal volume of acetonitrile). For LDTD, 2  $\mu$ L of sample was pipetted into each well and then dried. For ESI and APCI, flow injection was used to inject 5  $\mu$ L of sample into a flow rate of 1 mL/min of 50:50 water/acetonitrile containing 0.1% formic acid. The LDTD data showed good sensitivity and S/N ratios for all four CYP metabolites. Only dextrorphan showed 1.5–2-fold lower sensitivity than ESI and APCI. ESI and APCI appeared to be more sample dependent in their response. For ESI, 6 $\beta$ -hydroxytestosterone and acetaminophen showed 2–3 orders of magnitude lower signal and S/N than for LDTD. Dextrorphan worked well in ESI showing high sensitivity and high S/N. 4'-Hydroxydiclofenac had good signal intensity with ESI but the S/N was 260-fold lower than LDTD because of higher background. APCI achieved the best response

**Table 2. Comparison of Peak Areas, Reproducibility, and Signal-to-Noise Ratios of the Target Metabolites for LDTD, ESI, and APCI Using a Sciex API-4000 Mass Spectrometer<sup>a</sup>**

compound		ESI	APCI	LDTD
6 $\beta$ -hydroxytestosterone	peak area ( $\times 10^3$ )	38 $\pm$ 3.7	120 $\pm$ 8.2	1800 $\pm$ 280
	S/N	78	600	54000
dextrophan	peak area ( $\times 10^3$ )	2400 $\pm$ 170	3300 $\pm$ 300	1800 $\pm$ 42
	S/N	11000	27000	6600
4'-hydroxydiclofenac	peak area ( $\times 10^3$ )	935 $\pm$ 40	2400 $\pm$ 190	5700 $\pm$ 260
	S/N	107	4500	27000
acetaminophen	peak area ( $\times 10^3$ )	17 $\pm$ 3.9	7200 $\pm$ 240	12000 $\pm$ 1100
	S/N	53	5400	12000

<sup>a</sup> All the reported values were the average of triplicate 5  $\mu$ M samples in 0.25 mg/mL HLM protein solution (protein precipitated with equal volume of acetonitrile).

for dextrophan among the three ionization techniques and showed good responses for 4'-hydroxydiclofenac and acetaminophen although S/N was 2–6-fold lower than LDTD. 6 $\beta$ -Hydroxytestosterone did not yield good S/N ratios using flow injection APCI giving 90 $\times$  lower than LDTD. It is known that APCI is more tolerant against a matrix effect compared to ESI.<sup>27</sup> These data, together with results for other compounds, demonstrate that LDTD is tolerant of complex matrices such as HLM for a wide range of compound structural classes without the need for LC separation.<sup>28</sup> Of course, like any other technique, LDTD does not necessarily work for every compound. For example, because this source uses thermal desorption, compounds that thermally decompose rather than melt tend to give fragments instead of intact parent compound.

**Validation of LDTD-MS for Analysis of CYP Inhibition Assays.** The LDTD-MS technique uses no LC separation but relies on MS/MS specificity to differentiate different compounds. To apply the technique to complex mixture analysis, such as CYP inhibition assays, issues such as the potential for isobaric interferences and ion suppression must be addressed. The internal standards used in the assays were stable isotope-labeled analogues of the target metabolites with masses and fragment ions very similar to those of the metabolites. Isobaric interference was a concern when running pooled sample plates that contained all metabolites and internal standards. Interference was tested by using 5  $\mu$ M standards individually in HLM solution while scanning all metabolite and internal standard (IS) MRM channels simultaneously. None of the samples tested showed interferences in their MRM channels, but some did show interference from blank HLM samples. The problem was remedied by selecting a different product ion for the metabolite or IS. The list of compounds and their MRM transitions are listed in Table 1.

The CYP inhibition assay measures enzyme activity through quantification of the turnover of probe into metabolite. Metabolite levels were quantified using metabolite peak areas and compared to no inhibitor control samples (100% enzyme activity) and no inhibitor/no NADPH control samples (0% enzyme activity). Since the accuracy of the assay relies on the peak area of the metabolite, the potential for ion suppression of the metabolite was assessed.

Mixtures of metabolites and internal standards were prepared in HLM solution and spiked with known CYP inhibitors (zafirlukast, miconazole, or quinidine) at concentrations of 0, 0.2, 2, 20, and 200  $\mu$ M. Ion suppression of the metabolite by the inhibitor was found to be <30% with IS correction across all metabolites. The peak area/IS area ratio was normalized to a value of 1 for 6 $\beta$ -hydroxytestosterone with no inhibitor. The ratio was found to be 0.87 (13% suppression) with 200  $\mu$ M zafirlukast, 0.96 (4% suppression) with 200  $\mu$ M miconazole, and 1 (no suppression) with 200  $\mu$ M quinidine. The plate design for the CYP assay contains a well to test for inhibition containing the maximum concentration of the test compound and the metabolite of the probe substrate. To date, suppression of metabolite response has not been used to reject a data set.

It is known that the major metabolite of testosterone in HLM incubations under oxidative conditions is 6 $\beta$ -hydroxytestosterone. It has also been reported that other hydroxylated metabolites can be formed in HLM as minor products, such as 2 $\beta$ -, 15 $\beta$ - and 1 $\beta$ -hydroxytestosterone.<sup>29,30</sup> An assay was performed to test the specificity of CYP3A4 to produce 6 $\beta$ -hydroxytestosterone from testosterone in HLM in the presence of a CYP3A4 mAb.<sup>26</sup> A control antibody containing IgG prepared against non-CYP-related proteins was used as the negative control. Two separate concentrations of HLM were examined, 0.25 and 1 mg/mL, with an incubation time of 10 min (same as in the CYP3A4 inhibition assay). The samples were analyzed using UPLC-QTOF in the full scan mode. Accurate mass window of 0.02 Da around the exact mass of 6 $\beta$ -hydroxytestosterone (305.212 Da) was used to generate an extracted ion chromatogram for this and other potential hydroxylated metabolites. The resulting chromatograms (data not shown) for both concentrations of HLM in the control antibody incubation samples showed 6 $\beta$ -hydroxytestosterone as the major product (confirmed with 6 $\beta$ -hydroxytestosterone standard) along with three other hydroxylated metabolites (identity not confirmed with standards). In the 0.25 mg/mL HLM solution (same concentration as in the CYP3A4 inhibition assay), the 6 $\beta$ -hydroxytestosterone accounted for 84% of the total signal, and in the 1

(27) King, R.; Bonfiglio, R.; Fernandez-Metzler, C.; Miller-Stein, C.; Olah, T. *J. Am. Soc. Mass Spectrom.* **2000**, *11*, 942–950.

(28) Bateman, K. P.; Picard, P.; Mellon, C.; Letarte, S. Heat and Serve: Rapid Pharmacokinetics Using a Laser Diode Thermal Desorption (LDTD) Ion Source for Mass Spectrometry. Abstracts of the 54th ASMS Conference, Seattle, WA, 2006.

(29) Yamazaki, H.; Shimada, T. *Arch. Biochem. Biophys.* **1997**, *346*, 161–169.

(30) Krauser, J. A.; Voehler, M.; Tseng, L.-H.; Shefer, A. B.; Godejohann, M.; Guengerich, F. P. *Eur. J. Biochem.* **2004**, *271*, 3962–3969.

(31) von Moltke, L. L.; Greenblatt, D. J.; Duan, S. X.; Schmider, J.; Kudchadker, L.; Fogelman, S. M.; Harmatz, J. S.; Shader, R. I. *Psychopharmacology* **1996**, *128*, 398–407.

(32) Niwa, T.; Inoue-Yamamoto, S.; Shiraga, T.; Takagi, A. *Biol. Pharm. Bull.* **2005**, *28*, 1813–1816.

mg/mL HLM solution, it accounted for ~80% of the signal. In the incubation samples that contained the anti-CYP3A4 mAB, >99% inhibition was observed for 6 $\beta$ -hydroxytestosterone in the 0.25 mg/mL HLM protein sample and no other metabolites were detected. The 1 mg/mL HLM protein sample containing the CYP3A4 mAB showed 100% inhibition of 6 $\beta$ -hydroxytestosterone while another metabolite remained at ~4.5%. This confirmed that 6 $\beta$ -hydroxytestosterone was the major metabolite of testosterone produced in HLM and also that CYP3A4 was the major enzyme responsible for all the hydroxylated metabolites produced in HLM under the current CYP3A4 inhibition assay conditions. Therefore, even though LDTD-MS does not separate different hydroxylated metabolites, the total activity of CYP3A4 can still be effectively measured. This experiment would have to be repeated if a different batch of HLM is used for the CYP 3A4 inhibition assay.

A concern with the CYP 1A2 assay was the in-source fragmentation of the probe phenacetin to the metabolite acetaminophen. This was usually observed in the LC–MS chromatogram using ESI as the ionization technique. The concentration of phenacetin used in the incubation plates was 100  $\mu$ M. The expected turnover of phenacetin to acetaminophen by CYP 1A2 was estimated to be ~3% from the LC–MS assay. To address this problem, we compared the contribution from in-source fragmentation of a 100  $\mu$ M phenacetin standard with the MS signal of a 3  $\mu$ M acetaminophen standard (both prepared in HLM) using the LDTD-MS method. The contribution from in-source fragmentation of phenacetin on the acetaminophen channel was found to be only 3.7% of the signal obtained from the 3  $\mu$ M acetaminophen standard alone. A comparison of the minimum control in the CYP1A2 inhibition assay (no NADPH, maximum concentration of phenacetin, and no formation of acetaminophen), with the maximum control (+NADPH, no inhibitor, maximum amount of acetaminophen) was also done. The ratio was only 2.5% when comparing the acetaminophen peak areas from the minimum control to the maximum control. Both experiments showed minimal interference from in-source fragmentation of phenacetin in the LDTD-MS method.

Further validation of the LDTD-MS method was tested by comparing inhibition data obtained by LDTD-MS to data from a validated LC–MS method. Eighteen different drugs and 15 Merck compounds were tested in the competitive CYP inhibition assays. Samples from CYP 1A2/2C9/2D6/3A4 competitive inhibition assays were pooled and analyzed with LC–MS. Pooled plates were prepared by combining 20  $\mu$ L from each of the 1A2, 2C9, 2D6, and 3A4 quenched incubations with 160  $\mu$ L of water. Individual incubation plates for 1A2, 2C9, 2D6, and 3A4 were diluted 5 $\times$  in acetonitrile before being analyzed on the LDTD-MS.

The LC–MS method required 5.5 min per sample plus injector cycle time for a total data analysis time of more than 10 h for the pooled samples. Data obtained on the LC–MS were integrated and interpreted using Analyst quantitation software. For the LDTD-MS approach, each plate required 30 min with manual acquisition for a total of 30 min for pooled and 2 h if all four assay plates are run individually. In contrast to the LC–MS method, for LDTD-MS data were collected into a single file per 96-well plate and were analyzed directly by integrating the entire data file or by using MaldiQuan software. In addition, when running

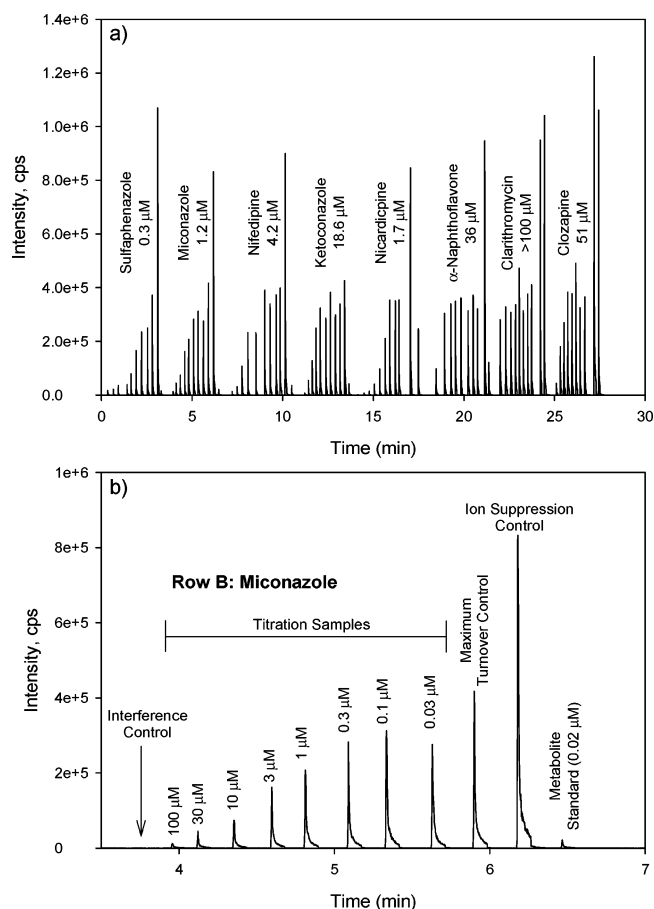


**Figure 5.** (a) Raw LDTD-APCI-MS data for sulfaphenazole, miconazole, nifedipine, ketoconazole, nicardipine,  $\alpha$ -naphthoflavone, clarithromycin, and clozapine titrations in the CYP2C9 inhibition assay (96 wells in <30 min). Each peak represents the signal generated by the presence of 4'-hydroxydiclofenac from CYP 2C9-mediated metabolism of diclofenac or from the metabolite in the control/standard curve wells. Values below each compound name represent experimentally determined  $IC_{50}$ 's. (b) Expansion of the data obtained for the analysis of row B (titration of miconazole). Values above titration samples represent concentration of test compound.

in the fully automated mode, the analysis time for a 96-well plate is further reduced to ~18 min.

Figure 5a depicts the raw LDTD-MS data from the analysis of a 96-well Lazwell plate containing sulfaphenazole, miconazole, nifedipine, ketoconazole, nicardipine,  $\alpha$ -naphthoflavone, clarithromycin, and clozapine titration samples from the CYP 2C9 competitive inhibition assay as well as controls and standards. Each peak represents the signal generated by the presence of 4'-hydroxydiclofenac from CYP 2C9-mediated metabolism of diclofenac or from the metabolite in the control/standard curve wells. Inhibition for individual compounds was easily visualized from the LDTD-MS total ion current. For example, a potent CYP 2C9 inhibitor such as miconazole shows a low signal for 4'-hydroxydiclofenac for the first several titration points (Figure 5b). These samples contain higher concentrations of miconazole, resulting in inhibition of CYP 2C9 mediated 4'-hydroxydiclofenac formation. In contrast, a compound such as clarithromycin, which is not an inhibitor of CYP 2C9, shows a strong signal for 4'-hydroxydiclofenac at all the samples in the titration curve. The layout for each row of the plate is shown in Figure 5b. The first well is the interference



**Table 3. Comparison of CYP IC<sub>50</sub> Values of Commercial Compounds from Competitive Inhibition Assays Measured by LD<sub>TD</sub>-MS and LC-MS**

compound	CYP	IC <sub>50</sub>		
		LD <sub>TD</sub>	LC-MS	literature
miconazole	2C9	1.2	1.1	0.13–4 <sup>10,14</sup>
	2D6	7.4	9.3	6.46 <sup>32</sup>
	3A4	0.23	0.13	0.10–0.2 <sup>11,15</sup>
ketoconazole	2C9	18.6	11.5	7.8–42 <sup>10,14</sup>
	3A4	0.03	0.03	0.023–0.26 <sup>11,14,15</sup>
nicardipine	2C9	1.7	1.5	0.28 <sup>10</sup>
	2D6	9.4	8.4	na <sup>a</sup>
	3A4	0.49	0.23	0.21–2 <sup>11,15</sup>
nifedipine	2C9	4.2	4.2	4.6 <sup>10</sup>
	3A4	16.3	3.4	11.5–48 <sup>11,14,15</sup>
mifepristone	2D6	9.4	9.6	na
	3A4	4.5	3.1	nan
clarithromycin	2C9	>100	>100	na
	3A4	>100	>100	na
α-naphthoflavone	1A2	0.06	0.07	0.02 <sup>14</sup>
	2C9	36	44	4–6 <sup>10,14</sup>
	2D6	>10	>10	na
quinidine	3A4	>10	>10	na
	1A2	>10	>10	>80 <sup>31</sup>
	2D6	0.18	0.19	0.02–0.24 <sup>2,4,14</sup>
clozapine	3A4	>10	>10	na
	1A2	>100	>100	na
	2C9	51	68	na
imipramine	2D6	22	42	8.19–29 <sup>2,14</sup>
	3A4	75.5	>100	na
	2D6	13	28	5.58 <sup>2</sup>
desipramine	2D6	11.5	9.4	2.21 <sup>2</sup>
	1A2	85	>100	na
bufuralol	2D6	20.7	23.8	8.97 <sup>2</sup>
	2C9	0.3	0.2	0.26–1.5 <sup>4,10,14</sup>
sulfaphenazole	1A2	1.0	0.5	0.24 <sup>31</sup>
fluvoxamine	1A2	79	50	na
genistein	1A2			

<sup>a</sup> na, not available.

control for each compound, containing 10 μM test compound and all incubation components except for the probe substrate. This allows for testing of interferences arising from the test compound and incubation components that may result in false positive detection of metabolite signal. The next eight wells are the titration samples ranging from 0.03 to 100 μM test compound. Sample column 10 contains the maximum (rows 1–4) and minimum (rows 5–8) turnover controls. Column 11 contains the ion suppression control with 100 μM test compound in the presence of 1.5 μM CYP 2C9 probe metabolite. This control well permits assessment of the potential for the metabolite signal to be reduced in the presence of the test compound. Column 12, rows 1–8, contains the metabolite standards at four different concentrations in duplicate wells. The IC<sub>50</sub> values obtained from LD<sub>TD</sub>-MS (e.g., 1.2 μM for miconazole) and LC-MS (1.1 μM for miconazole) were in good agreement with each other and the literature value for miconazole of 0.13–4 μM.<sup>10,14</sup>

Tables 3 and 4 list the IC<sub>50</sub> values of all the compounds tested in the competitive inhibition assays for CYP1A2, CYP2C9, CYP2D6 and CYP3A4. The IC<sub>50</sub> values from the LD<sub>TD</sub>-MS and the LC-MS generally agree with each other within 2-fold. The experimental IC<sub>50</sub> values were also in good agreement with the literature values, when available. The correlation plot between the IC<sub>50</sub> values obtained from LD<sub>TD</sub>-MS and LC-MS is shown in Figure 6. Regression analysis shows a linear equation of  $y = 0.9048x$  with

**Table 4. Comparison of CYP IC<sub>50</sub> Values of Merck Compounds from Competitive Inhibition Assays Measured by LD<sub>TD</sub>-MS and LC-MS**

compound	CYP	IC <sub>50</sub>	
		LD <sub>TD</sub>	LC-MS
Merck-1	1A2	>100	>100
	2C9	37	31
	2D6	43	40
Merck-2	3A4	0.4	0.7
	1A2	>100	>100
	2C9	16	38
Merck-3	2D6	20	31
	3A4	9.0	7.0
	1A2	>100	>100
Merck-4	2C9	52	54
	2D6	26	21
	3A4	3.0	3.0
Merck-5	1A2	>100	>100
	2C9	42	40
	2D6	>100	>100
Merck-6	3A4	9.0	11.0
	1A2	>100	>100
	2C9	57	61
Merck-7	2D6	>100	>100
	3A4	5.0	16.0
	1A2	>100	>100
Merck-8	2C9	6.5	5.5
	2D6	38	58
	3A4	16.7	30.0
Merck-9	1A2	>100	>100
	2C9	6.8	5.0
	2D6	>100	>100
Merck-10	3A4	16.3	9.6
	1A2	>10	>10
	2C9	1.4	1.2
Merck-11	2D6	>10	>10
	3A4	>10	>10
	1A2	>30	>30
Merck-12	2C9	>30	>30
	2D6	>30	>30
	3A4	>30	>30
Merck-13	1A2	>100	>100
	2C9	17.3	17.7
	2D6	>100	>100
Merck-14	3A4	>100	>100
	1A2	20	10
	2C9	5.6	4.7
Merck-15	2D6	25.7	29.9
	3A4	24.0	23.3
	1A2	>100	>100
Merck-16	2C9	46.6	31.7
	2D6	>100	>100
	3A4	37.0	31.1
Merck-17	1A2	>100	>100
	2C9	7.1	5.6
	2D6	93	68
Merck-18	3A4	>100	>100
	1A2		

an  $r^2$  value of 0.94, whereas the plot shows the line with a slope of unity. This result demonstrates that LD<sub>TD</sub>-MS provides a reliable measurement of the potency (IC<sub>50</sub>) of CYP 1A2/2C9/2D6/3A4 inhibitors relative to an internal Merck validated LC-MS assay. The comparisons between the LC-MS and LD<sub>TD</sub>-MS methods show the use of the LD<sub>TD</sub> in place of an LC system for



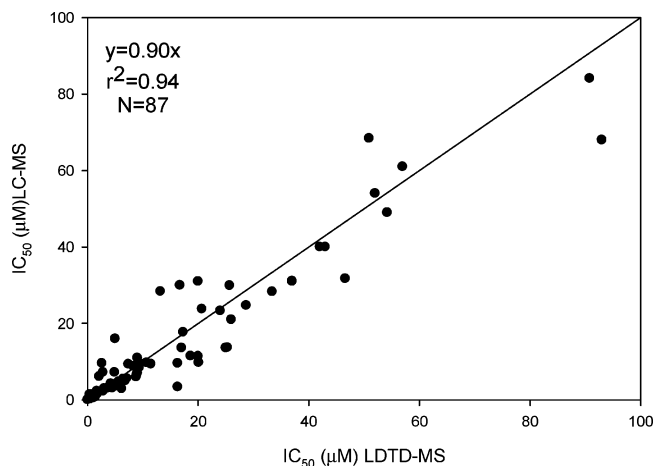


**Figure 6.** Correlation plot between the  $IC_{50}$  values obtained from LDTD-APCI-MS and LC-MS methods ( $N = 87$ ).

CYP inhibition analysis will garner comparable results while allowing for a significant increase in sample throughput.

## CONCLUSIONS

A high-throughput, sensitive, and reproducible method for the analysis of CYP 1A2/2C9/2D6/3A4 inhibition assays has been developed using a sample introduction method based on thermal

desorption and mass spectrometry. Optimization of laser power and time, as well as carrier gas flow rate, was shown to be important parameters for method development. Issues specific to the CYP assay were also addressed including the potential for interferences, in-source fragmentation, and the contribution of non-CYP 3A4 metabolism on the assay. The results demonstrate that the use of the LDTD-APCI ion source can reduce analysis time from  $\sim 10$  h to  $< 30$  min for a 96-well plate without compromising assay sensitivity or accuracy over a previously validated LC-MS/MS method. When compared to current high-throughput methods (0.5–1 min cycle times), this approach is 300–600% faster, has reduced solvent consumption, and no carryover as each sample is analyzed directly. To further improve throughput, a modified version of the LDTD source has recently been completed providing the ability to load 10 sample plates for continuous operation without user intervention. In the future, the ability to analyze 384-well plates is anticipated to further enhance sample throughput.

Received for review February 2, 2007. Accepted April 4, 2007.

AC070221O